

Performance of Photovoltaic Thermal Collector (PVT) With Different Absorbers Design

ADNAN IBRAHIM*, M.Y. OTHMAN, M.H. RUSLAN,
M.A. ALGHOUL, M.YAHYA, AND A. ZAHARIM AND K. SOPIAN
Solar Energy Research Institute,
Universiti Kebangsaan Malaysia,
43600, Bangi, Selangor.
MALAYSIA

adnan@vlsi.eng.ukm.my*, ksopian@vlsi.eng.ukm.my, myho@ukm.my,
hafidz@ukm.my, dr.alghoul@gmail.com, azaminelli@gmail.com

Abstract: - Much effort has been spent on the development of hybrid PVT, in order to improve its efficiency of both, thermal and cell. The combination of thermal and cell efficiencies, which is commonly known as “total efficiency of the PVT”, is influenced by many system design parameters and operating conditions. Due to that, seven new design configurations of absorber collectors are designed, investigated and compared. Simulations were performed to determine the best absorber design that gives the highest efficiency (total efficiency). In these simulations, the system is analyzed with various parameters, such as solar radiation, ambient temperature, and flow rate conditions. It is assumed that the collector is represented as a flat plate thermal collector with single glazing sheet. Based on these simulations, spiral flow design proved to be the best design with the highest thermal efficiency of 50.12% and corresponding cell efficiency of 11.98%.

Key-Words: - Photovoltaic Thermal (PVT), thermal and cell efficiency, absorbers collector, Design

1 Introduction

With the concern of global crisis on utilization of energy resources such as oil and gas, PVT has become an important research area to receive much more attention. PVT system collector consists of the Photovoltaic systems for the electricity generated and thermal collectors system for the hot water generated. Combining both systems provided great advantages, such as:

1. Minimized the usage of the installation area, the installation area produces more energy per unit surface area than one PV panel and one hot water system. (Sopian *et al.* [1996])
2. Attractive in case of the available roof surface is limited.
3. Replacing the roofing material with the PVT system can reduce the payback period.

One of the limitations of the system is due to its high cost over the low efficiency. It is believed that, due to the increasing of solar radiation, the temperature of the PV module will increase, simultaneously decreases its electrical efficiency. Tripanagnostopoulos *et al.* [2002]. New method

need to be produced enable to achieve higher efficiency and simultaneously lower the cost consumed. By increasing the efficiency of both systems, enable it be used as domestic applications. (Kalogirou *et al.* [2006]).

Research in this field has been carried out in the middle of 1970s to early 1980s. Zondag [2008], mentioned that the first inventor on the flat-plate PVT liquid system is Martin Wolf [1976] who analyzed the performance of combining the heating and photovoltaic power systems for residential applications. He concluded that the system was technically feasible and cost effective. In his experiment, the Hottel-Whillier (Hottel [1958]) model has been used to analyze the combination of photovoltaic/thermal flat plate collectors and the traditional hot water system with the PV panel to minimize the usage of the installation area while producing more energy per unit surface area.

Later, Zondag *et al.* [2003] examined nine different designs, ranging from the complicated to the simpler one, in order to investigate the maximum yield. They concluded that the design of the channel below the transparent PV, with PV-on-

sheet and tubes design gives the best overall efficiency.

Bergene *et al.* [1995] performed theoretical examination of a flat plate solar collector model that integrated with solar cells and developed a series of algorithms for making quantitative predictions for both, electrical and thermal efficiencies, which resulting efficiency in the range of 60-80%.

Group of researchers, Chow *et al.* [2005]; He *et al.* [2006]; and Ji *et al.* [2007] have developed and experiment the PV/T collector. In their experiments, a flat plate collector is used, which is comprised of glass cover (glazed) and solar cell. Underneath the solar cell, they inserted the encapsulated materials, such as transparent TPT (tedlar – polyester - tedlar) and the EVA (ethylene – vinyl acetate). The absorber plate with flat box channel was built from multiple of extruded aluminum alloy box structure modules, which were assembled to produce a flat smooth top surface. They used natural convection to circulate the water and the result showed a combined efficiency of 50% to the system, with daily thermal efficiency of 40%.

Fujisawa *et al.* [1997] have developed a flat plate collector using a single cover system. In their design, they constructed the coverless PV/T collector in order to produce higher electrical output by decreasing the optical loss. It comprised of flat box with glass cover on top, solar cell, absorber in the form of aluminum roll bond absorber plate with fluid conduit. Underneath the absorber plate, the glass wool was used as a heat insulating material.

Huang *et al.* [2001] have developed PV/T system using a polycrystalline solar PV module, adopted to be combined with a collector plate. The collector plate is directly contact with the commercial PV module using thermal grease, for better contact. Underneath the collector, a PU thermal insulation layer is attached using a fixing frame. The collector was designed using the corrugated plate made of polycarbonate material. The water was flowed in the flow channel of the corrugated plate structure.

Kalogirou *et al.* [2007] designed the hybrid PV/T solar systems for domestic hot water and electrical using the poly-crystalline silicon (pc-Si) and amorphous silicon (a-Si) module type that combined with the solar collector plate. In their design, they have employed the typical flat plate of solar collector, as shown in Figure 4. The absorber plate, which utilized the copper material, acts as a heat removal medium to the design. The transparent cover is used in this experiment. The purpose of the transparent cover is twofold. Firstly, to reduce the

conduction losses from the absorber plate through the restraint of the stagnant air layer between the absorber and the glass and secondly, to reduce the radiation losses from the collectors.

2 Design Configurations of the Absorber Collectors

The collector conceptual designs, as shown in Figs 1 – 7, comprised of seven new design configurations. Table 1 shows the parameters of the absorber collectors design. The absorbers in the form of round and rectangular hollow tubes are attached closely underneath the PV module with metallic bonded; this will ensure a zero gap or no gap between the tubes and the module, in which heat can be transferred. Rockendorf *et al.* [1999] and later Chow [2003] have discovered that the fin efficiency and bonding quality between the collector and the sheet underneath the cell (module), as the crucial factors, which often bring limitations to the overall efficiency achievable.

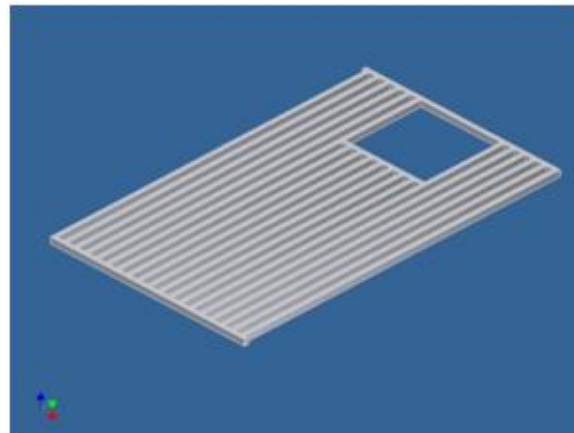


Fig.1: Direct Flow Design

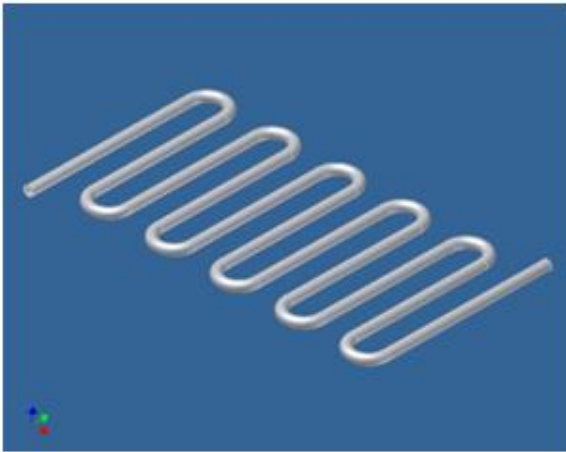


Fig.2: Oscillatory Flow Design

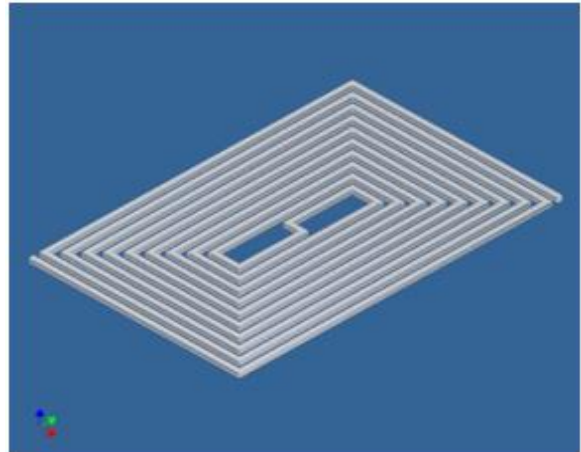


Fig.4: Spiral Flow Design



Fig.3: Serpentine Flow Design

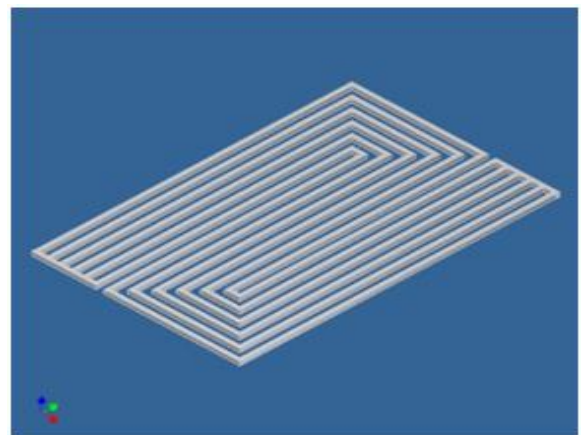


Fig.5: Parallel-Serpentine Flow Design

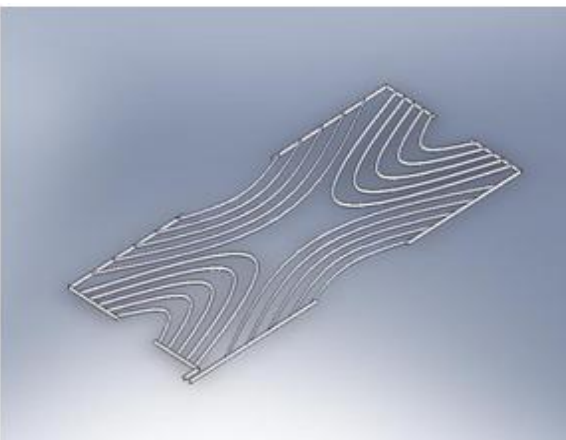


Fig.4: Web Flow Design

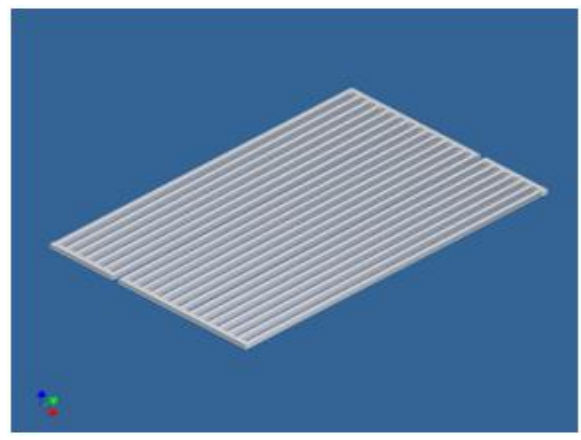


Fig.6: Modified Serpentine-Parallel
Flow Design

Table 1: Parameters of the absorber collectors design

Fig.1: Direct flow	Absorber material: rectangular hollow tubes of Stainless steel Absorber collector module: 19 channel each of size 12.7 mm x 12.7 mm x 1mm x 1000 mm (L) and 640 mm (W) Method of joining: welding Inlet/Outlet no: 4
Fig.2: Oscillatory flow,	Absorber material: round hollow tubes of Stainless steel
Fig.3: Serpentine flow, and Fig.4: Web flow	Absorber collector module: 1 channel each of size Ø12.7 mm x 1 mm x 1000 mm (L) and 640 mm (W) Method of joining: welding Inlet/Outlet no: 2
Fig.5: Spiral flow	Absorber material: rectangular hollow tubes of Stainless steel Absorber collector module: 1 channel each of size 12.7 mm x 12.7 mm x 1 mm x 700 mm (L) and 640 mm (W) Method of joining: welding Inlet/Outlet no: 4
Fig.6: Parallel-Serpentine flow, and Fig.7: Modified Serpentine-Parallel flow	Absorber material: rectangular hollow tubes of Stainless steel Absorber collector module: 6 channel each of size 12.7 mm x 12.7 mm x 1 mm x 700 mm (L) and 640 mm (W) Method of joining: welding Inlet/Outlet no: 2

As the PV cells in PV module are exposed the sun, it generates electricity and at the same time absorbed the heat causing the absorber to increase its temperature. During this time, the water fluid passing inside the absorber tubes is heated due to the contact underneath the PV module. The water is then flows along the absorber through a manifold and pipes before finally fed to a water tank. Water,

which is used as a cooling agent, flows at 0.01 kg/s continuously inside the hollow tubes.

The absorbers are equipped with inlet and outlet at opposite ends of the hollow tubes. This will ensure that the trapped air in the absorber can be releases. The system is considered to be a closed loop system, where the fresh and cooler water enters the hollow tubes is heated continuously. Result of the continuous operation of the flowing water consequently reduces the temperature of the PV cells and simultaneously increasing it efficiency (for mono and poly crystalline silicon cells). A schematic overview of the system is shown in Fig 8.

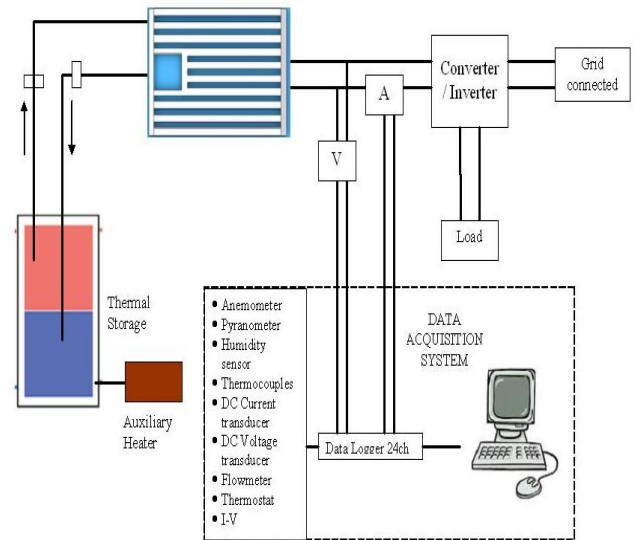


Fig.8 Schematic overview of the system

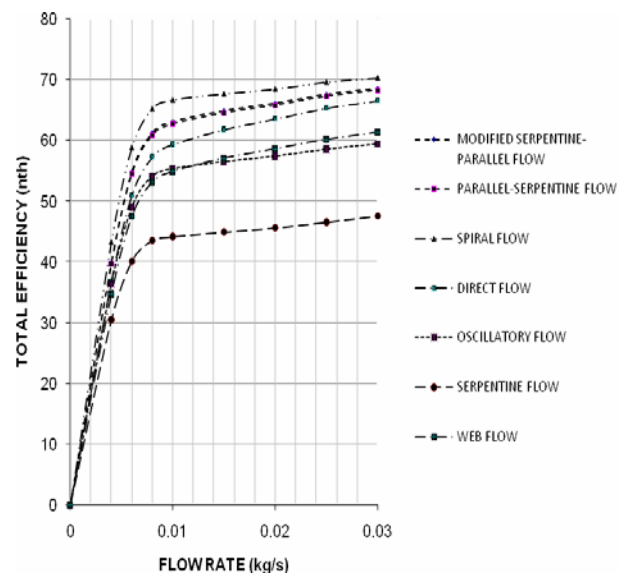


Fig.9 Flow rates configurations of various absorber collectors.

3 Parameters for Simulation Model

The absorber collector simulations are performed using Microsoft Excel software. In the simulation, data collection is set from 06.00 till 20.00 hours. The system parameters for inputs in the simulation model are shown in Table 2.

Table 2: System parameters for inputs to the simulation design

Polycrystalline silicon solar module	Tilt angle: 14° facing south Thickness: 0.004 m Total effective area: 0.65m ² Emissivity: 0.8 Number of Glass Covers: 1 Emittance of Glass: 0.88 Emittance of Plate: 0.95 Coefficients: 0.7037023
Heat Transfer Coefficients	Fluid flow rate: 0.01 kg/s Heat transfer coefficient from cell to absorber: 45 Heat transfer coefficient inside tube: 333.3781731
Back insulation layer	Thickness: 0.003m Back insulation conductivity: 0.045 (W/m°C) Back insulation thickness: 0.05m Insulation Conductivity: 0.045 Edge Insulation Thickness: 0.025m Absorber Conductivity: 51 Fin Conductivity: 84 Fin thickness: 0.0005m Back loss coefficient: 0.9

4 Theoretical Analysis

The performance of PVT collectors can be depicted by the combination of efficiency expression. (He *et al.* [2006]). It comprised of the thermal efficiency η_{th} and the electrical efficiency η_e , which usually include the ratio of the useful thermal gain and electrical gain of the system to the incident solar irradiation on the collector's gap within a specific time or period. The total efficiency η_o is used to evaluate the overall performance of the system:

$$\eta_o = \eta_{thermal} + \eta_{electrical} \quad (1)$$

The thermal performance of the PVT is affected by many system design parameters and operating conditions. In this simulation, the system is analyzed with various configurations of solar radiation, ambient temperature, and flow rate conditions. It is also assumed that the collector is represented as a flat plate thermal collector with single glazing sheet.

The thermal performance η_{th} of the PVT unit is evaluated for its thermal and photovoltaic performance, as such, the derivation of the efficiency parameters based on the Hottel-Whillier equations (Hottel [1958]) were used.

The thermal efficiency (η_{th}) of the conventional flat plate solar collector is calculated using the formula below:

$$\eta_{th} = \frac{\text{Useful Output}}{\text{Solar Input}} = \frac{Q}{G} \quad (2)$$

Under these conditions, the useful collected heat (Q) is given by:

$$\dot{Q} = \dot{m} C_p (T_a - T_i) \quad (3)$$

The difference between the absorber solar radiation and thermal heat losses is identified as:

$$\dot{Q} = A_c F_R [S - U_L (T_i - T_a)] \quad (4)$$

From the Eq (3), the S is identified as:

$$S = (\tau\alpha)_{pV} G_T \quad (5)$$

The heat removal efficiency factor (F_R) can be calculated as:

$$F_R = \frac{m C_p}{A_c U_L} \left[1 - \exp \left[- \frac{A_c U_L F'}{m C_p} \right] \right] \quad (6)$$

The corrected fin efficiency (F') is calculated using:

$$F' = \left[\frac{\frac{1}{U_L}}{U_L(d_h + (W - d_h)F)} \right] + \frac{1}{C b_{pV}} + \frac{1}{2(a+b)h_f} \quad (7)$$

The fin efficiency factor F is then calculated as:

$$F = \frac{\tanh \left(m \left(\frac{W - d_h}{2} \right) \right)}{\sqrt{m \left(\frac{W - d_h}{2} \right)}} \quad (8)$$

Where m :

$$m = \sqrt{\frac{U_L}{K_{abs} \cdot L_{abs} + K_{pV} \cdot L_{pV}}} \quad (9)$$

From these equations, it is then possible to calculate the useful heat gain by the solar collector. By rearranging Eq (2), the thermal efficiency of the collector is expressed as: (Vokas *et al.* [2006])

$$\eta_{th} = F_R (\tau\alpha)_{pV} - F_R U_L \frac{T_i - T_a}{G_T} \quad (10)$$

For temperature-dependent electrical efficiency of the PV module, (η_e) Tiwari *et al.* [2006], the expression is given as below:

$$\eta_e = \eta_r [1 - \beta(T_c - T_r)] \quad (11)$$

From the Eq. 10, the values of $F_R U_L$ and $F_R (\tau\alpha)_{pV}$ of the thermal and cell efficiency curve of various configuration of PVT collectors are presented in Fig. 10 and 11.

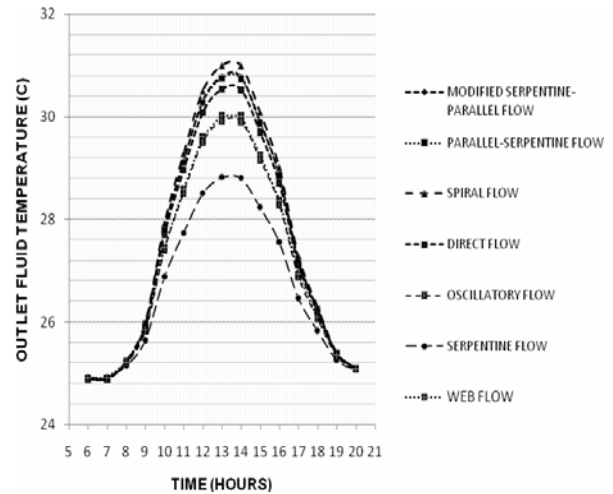


Fig.10 Variation of water temperature (output) versus the time of various absorber collectors

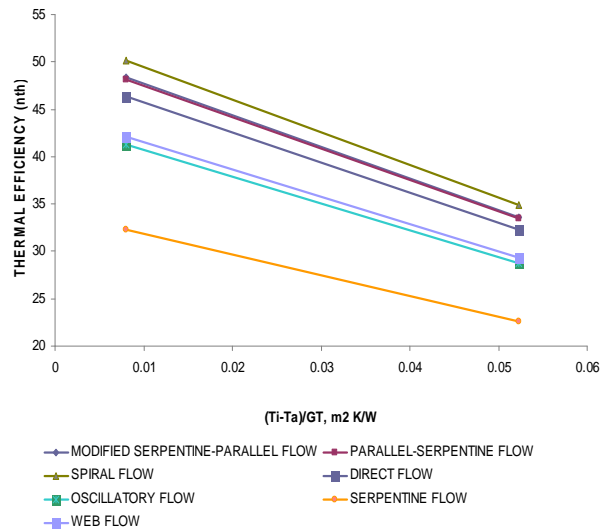


Fig.11 Thermal efficiency of various absorber collectors.

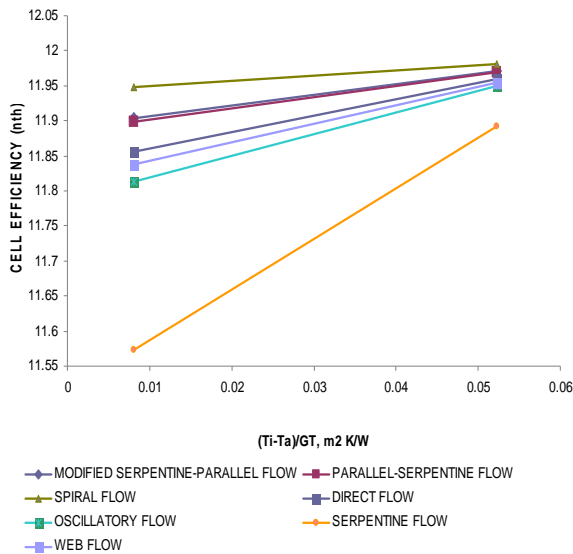


Fig.12 Cell efficiency of various absorber collectors.

5 Simulation Results

In this simulation, the effect on efficiency is minimal when the flow rate has reached certain values. As seen in Fig 9 the total efficiency is almost constant once the flow rate reaches 0.01kg/s. Further increase of the flow rate shows insignificant increase of the system total efficiency. This will only increase the energy used and its cost. As a result, the value of the flow rate is considered to be optimized during the production of the actual module. Spiral flow design obtained the highest total efficiency (68%) while Serpentine flow design having the lowest total efficiency of 45%.

Fig. 10 shows variation output of water temperature from the absorber collectors versus time. In this simulation, it is noted that the Spiral flow design gave the highest output temperature of 31°C between 1300 and 1400 hours, which is the highest temperature recorded in a day, (The highest temperature recorded is at 1400 hour with 36.1°C and water temperature is at 25°C) followed by the Modified Serpentine-Parallel flow with 30.7°C, Parallel Serpentine flow with 30.5°C, Direct flow with 30.3°C, Web flow with 29.5°C, Oscillatory flow with 29.9°C and lastly by Serpentine flow with 28.8°C. The differences of the output temperature are due to the design configuration of the absorber.

The first four absorbers, which are Spiral flow, Modified Serpentine-Parallel flow, Parallel Serpentine flow and Direct flow have been designed with smaller (tight) spacing between the tubes (W) as in Eq.(7), while the other design such as Web

flow, Oscillatory flow and Serpentine flow have slightly larger spacing gap between the tube (W).

It is believed that the closer the spacing gap covered by the entire PV module, the more heat can be absorbed. This concurrently can eliminate the heat generated and cooling the PV module and at the same time increases the efficiency of the photovoltaic and thermal systems.

Based on the Figs. 11 and 12, the thermal and cell efficiency of the PV module can be expressed in terms of the inlet temperature T_i , the ambient temperature T_a , and the incoming solar-irradiation on the collector surface G_T . Bakker *et al.* [2005] as in Eq.(10). The calculated thermal and cell efficiency of PVT collector with reduced temperature are shown in Fig 11 and 12.

The regression lines for thermal efficiency were found as follows:

$$\text{Fig 1 design: } \eta_{th} = 32.32 - 46.41 \frac{T_i - T_a}{G_T}$$

$$\text{Fig 2 design: } \eta_{th} = 28.74 - 41.24 \frac{T_i - T_a}{G_T}$$

$$\text{Fig 3 design: } \eta_{th} = 22.57 - 32.35 \frac{T_i - T_a}{G_T}$$

$$\text{Fig 4 design: } \eta_{th} = 29.37 - 42.15 \frac{T_i - T_a}{G_T}$$

$$\text{Fig 5 design: } \eta_{th} = 34.89 - 50.12 \frac{T_i - T_a}{G_T}$$

$$\text{Fig 6 design: } \eta_{th} = 33.51 - 48.12 \frac{T_i - T_a}{G_T}$$

$$\text{Fig 7 design: } \eta_{th} = 33.65 - 48.33 \frac{T_i - T_a}{G_T}$$

The regression lines for cell efficiency were found as follows:

$$\text{Fig 1 design: } \eta_{cell} = 11.85 - 11.95 \frac{T_i - T_a}{G_T}$$

$$\text{Fig 2 design: } \eta_{cell} = 11.81 - 11.94 \frac{T_i - T_a}{G_T}$$

$$\text{Fig 3 design: } \eta_{cell} = 11.57 - 11.89 \frac{T_i - T_a}{G_T}$$

$$\text{Fig 4 design: } \eta_{cell} = 11.83 - 11.95 \frac{T_i - T_a}{G_T}$$

$$\text{Fig 5 design: } \eta_{cell} = 11.94 - 11.98 \frac{T_i - T_a}{G_T}$$

$$\text{Fig 6 design: } \eta_{cell} = 11.89 - 11.96 \frac{T_i - T_a}{G_T}$$

$$\text{Fig 7 design: } \eta_{cell} = 11.90 - 11.97 \frac{T_i - T_a}{G_T}$$

For thermal efficiency, it is clearly shown that the Fig. 5 design of Spiral flow indicated the highest thermal efficiency compared to other design configurations. The collector efficiency factor in this simulation for Spiral flow design is 50.12% and the lowest is the Serpentine flow design of 32.35%. It is found that, not much change can be done for the cell efficiency. The highest cell efficiency recorded is Fig. 5 design of Spiral flow. The collector efficiency factor for cell efficiency of Spiral flow design is 11.98% and the lowest is Fig. 2 design of Oscillatory flow design at 11.94%.

6 Conclusions and Recommendation

A theoretical model was developed based on the present study, found that:

1. It is advisable to perform simulation software at early stage of design, to enable justification for the correct design configuration of any design proposed.
2. The gap or spacing (W) between the hollow tubes plays an important role in design configuration. It is recommended that the design should be consider as fully covered the surfaces underneath the PV module to enable obtaining good results.
3. From the simulation, it is proved that by setting the spacing (gap) to zero tolerance underneath the entire PV module, enable the heat to be absorbed and eliminate the heat generated, simultaneously cooling the PV module and increases the efficiency of the photovoltaic and thermal systems.
4. It is difficult to change the efficiency of cell due to its natural characteristics towards the heat. As in regression lines for cell proved that the efficiency for the cell is almost static. The only way to obtain the high efficiency of cell is by manipulating the design configuration of the

thermal to enable gaining total efficiency of the system.

5. The thermal and cell efficiency of the PVT collector can be further improved by using other types of cell such as the amorphous silicon cell with a higher absorption due to it black surfaces.
6. It is proven through mathematical model that the Fig 5 design of Spiral Flows having the highest thermal efficiency of 50.12% with corresponding cell efficiency of 11.98% is very much encouraging, considering the simple design of this collector type.

Nomenclature

A_c	Function of the collector area	m^2
C_b	Conductance of the bond between the fin and square tube	$W/(m K)$
C_p	Specific heat of the collector cooling medium	$J/kg K$
d_h	Hydraulic diameter	M
F	Fin efficiency factor	
F'	Corrected fin efficiency	
F_R	Heat removal efficiency factor	
G	Measured incoming solar-irradiation on the collector surface.	W/m^2
G_T	Solar radiation at NOCT (irradiance level $800 W/m^2$, wind velocity $1 m/s$, ambient temperature $26^\circ C$) (06:00 to 20:00)	
h_{fi}	Heat transfer coefficient of fluid	$W/m^2 K$
K_{ab}	Absorber thermal conductivity	$W/(m K)$
K_{pv}	Photovoltaic thermal conductivity	$W/(m K)$
η_r	Reference efficiency of PV module (0.12)	
L_{ab}	Absorber thickness	m
L_{pv}	PVT collector thickness	m
M	System flow rate	Kg/s
\dot{m}	Mass flow rate	Kg/s
\dot{Q}	Actual useful heat gain	W/m^2
S	Absorbed solar energy	W/m^2
T_c	Temperature of the solar cells	K

T_a	Ambient temperature	K
T_r	Reference temperature	
T_i	Fluid inlet temperature	K
U_L	Overall collector heat loss coefficient	$W/m^2 K$
W	Tube spacing	
	<i>Greek symbols</i>	
β	Temperature coefficient ($0.0045^\circ C^{-1}$)	$^\circ C$
$\tau\alpha$	Average transmittance-absorptance of the collector	
η_{th}	PV/T thermal efficiency	

7 Acknowledgment

The authors would like to express their gratitude to Universiti Kebangsaan Malaysia and the Ministry of Science, Technology and Innovation Malaysia for sponsoring the work under Science fund project 03-01-02-SF0039.

References:

- [1] Bakker, M., H. A. Zondag, M. J. Elswijk, K. J. Strootman, and M. J. M. Jong. Performance and costs of a roof-sized pv/thermal array combined with a ground coupled heat pump. *Solar Energy* 78 (2):331-339.2005
- [2] Bergene, Trond, and Ole Martin Lovvik. Model calculations on a flat-plate solar heat collector with integrated solar cells. *Solar Energy* 55 (6):453-462.1995
- [3] Chow, T. T. Performance analysis of photovoltaic-thermal collector by explicit dynamic model. *Solar Energy* 75 (2):143-152.2003
- [4] Chow, T. T., W. He, and J. Ji. Photovoltaicthermal collector system for domestic application. *Proceedings of Solar World Congress ISEC2005-76128 (ISES 2005)*.2005
- [5] Fujisawa, Toru, and Tatsuo Tani. Annual exergy evaluation on photovoltaic-thermal hybrid collector. *Solar Energy Materials and Solar Cells* 47 (1-4):135-148.1997
- [6] He, Wei, Tin-Tai Chow, Jie Ji, Jianping Lu, Gang Pei, and Lok-shun Chan. Hybrid photovoltaic and thermal solar-collector designed for natural circulation of water. *Applied Energy* 83 (3):199-210.2006
- [7] Hottel, H. C. and A Whillier. Evaluation of flat-plate solar collector performance. (*Trans. of the Conference on Use of Solar Energy*, 2, 74).1958
- [8] Huang, B. J., T. H. Lin, W. C. Hung, and F. S. Sun. Performance evaluation of solar photovoltaic/thermal systems. *Solar Energy* 70 (5):443-448.2001
- [9] Ji, Jie, Jian-Ping Lu, Tin-Tai Chow, Wei He, and Gang Pei. A sensitivity study of a hybrid photovoltaic/thermal water-heating system with natural circulation. *Applied Energy* 84 (2):222-237.2007
- [10] Kalogirou, S. A., and Y. Tripanagnostopoulos. Hybrid pv/t solar systems for domestic hot water and electricity production. *Energy Conversion and Management* 47 (18-19):3368-3382.2006
- [11] Kalogirou, S. A., and Y. Tripanagnostopoulos. Industrial application of pv/t solar energy systems. *Applied Thermal Engineering* 27 (8-9):1259-1270.2007
- [12] Rockendorf, Gunter, Roland Sillmann, Lars Podlowski, and Bernd Litzenburger. Pv-hybrid and thermoelectric collectors. *Solar Energy* 67 (4-6):227-237.1999
- [13] Sopian, K., K. S. Yigit, H. T. Liu, S. Kakac, and T. N. Veziroglu. Performance analysis of photovoltaic thermal air heaters. *Energy Conversion and Management* 37 (11):1657-1670.1996
- [14] Tiwari, Arvind, and M. S. Sodha. Performance evaluation of hybrid pv/thermal water/air heating system: A parametric study. *Renewable Energy* 31 (15):2460-2474.2006
- [15] Tripanagnostopoulos, Y., Th Nousia, M. Souliotis, and P. Yianoulis. Hybrid photovoltaic/thermal solar systems. *Solar Energy* 72 (3):217-234.2002
- [16] Vokas, G., N. Christandonis, and F. Skittides. Hybrid photovoltaic-thermal systems for domestic heating and cooling--a theoretical approach. *Solar Energy* 80 (5):607-615.2006
- [17] Wolf, Martin. Performance analyses of combined heating and photovoltaic power systems for residences. *Energy Conversion* 16 (1-2):79-90.1976
- [18] Zondag, H. A. Flat-plate pv-thermal collectors and systems: A review. *Renewable and Sustainable Energy Reviews* 12 (4):891-959.2008
- [19] Zondag, H. A., D. W. de Vries, W. G. J. van Helden, R. J. C. van Zolingen, and A. A. van

Steenhoven. The yield of different combined
pv-thermal collector designs. *Solar Energy* 74
(3):253-269.2003